HYUN-GYU LEE*,**, SANG-HOON CHOI*,**, JAE-JIN SIM*, JAE-HONG LIM*,**,
SOONG-KEUN HYUN**, JONG-HYEON LEE***, KYOUNG-TAE PARK*#

ELECTROREFINING OF INDIUM METAL FROM IMPURE In-Sn ALLOY IN FLUORIDE MOLTEN SALT

In this study, molten salt electrorefining was used to recover indium metal from In-Sn crude metal sourced from indium tin oxide (ITO) scrap. The electrolyte used was a mixture of eutectic LiF-KF salt and InF_3 initiator, melted and operated at 700°C. Voltammetric analysis was performed to optimize InF_3 content in the electrolyte, and cyclic voltammetry (CV) was used to determine the redox potentials of In metal and the electrolyte. The optimum initiator concentration was 7 wt% of InF_3, at which the diffusion coefficients were saturated. The reduction potential was controlled by applying constant current densities of 5, 10, and 15 mA/cm^2 using chronopotentiometry (CP) techniques. In metal from the In-Sn crude melt was deposited on the cathode surface and was collected in an alumina crucible.

Keywords: Indium metal, molten salt electrolysis, cyclic voltammetry, chronopotentiometry, electrodeposition

1. Introduction

Indium tin oxide (ITO), widely used as a transparent electrode material, has seen increasing demand due to recent developments in the electronic industry. Consequently, indium production is also steadily increasing because it is a main component of this industry. However, indium has no ores of its own; it is primarily produced as a by-product of the zinc and lead smelting processes [1]. Many efforts have been devoted to recover indium from ITO scrap due to its high utilization rates and high prices [2-3].

At present, the commercial recycling of ITO scrap involves a hydrometallurgical process. The ITO scrap is leached with strong acids like hydrochloric acid, nitric acid, and sulfuric acid, followed by processes such as solvent extraction and homogeneous liquid-liquid extraction (HOLLE), which are causing environmental degradation [3]. The molten salt electrolytic refining process consumes less energy than the commercial indium metal recycling process, and can extract metal directly from the metal phase. It can also reduce the emission of CO_2 and toxic gases, and the used electrolyte can be recycled, making it an inexpensive and environment-friendly process [4].

The molten salt is an ionic liquid melted at comparatively higher temperatures than aqueous salts, and contained metal ions as ionic phases. Molten salts are used in various fields like the production of alkali metals and light metals, high-melting-point rare metals like Ti and Zr, in uranium production, etc. [4-10], and are also used in recycling nuclear fuel [11]. For Ti, Zr, U, and Nd, the molten salt electrolytic refining process is performed for the production of high-purity materials using the crude metal as the typical solid-phase anode. The anode is electrochemically dissolved by applying external electrochemical force and is then deposited onto the cathode [4-11]. However, when using solid anodes, if the electrolyte contains oxides, passivation occurs on the anode surface and the current efficiency is decreased.

Use of the anode in liquid metal form can prevent deterioration of the current efficiency, and stable electrodeposition can be performed with excellent impurity separation and prevention of overvoltage [12]. If the deposit is recovered as a liquid metal, handling the collected metal is easier and may not be disturbed by changes in the cathode in the electrorefining process. Liquid-type electrodes have also been reported to suppress the reaction between the cathode material and the electrodeposit; alloy production is also easier during electrolysis when we choose liquid electrodes [12].

Herein we propose a process of recovering In metal by electrorefining from In-Sn alloys obtained from ITO, which could reduce environmental problems associated with commercial processes. We investigated the possibility of recovering In metal via molten salt electrolytic refining of a liquid In-Sn alloy produced by molten salt electrolytic smelting of waste ITO. Cyclic voltammetry (CV) experiments were performed to confirm the LiF-KF molten salt and oxidation and reduction potentials of In^{3+} ion. In this process, the reaction of In^{3+} at the
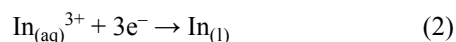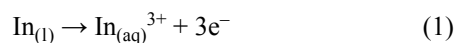
*   KOREA INSTITUTE OF INDUSTRIAL TECHNOLOGY, INCHEON, REPUBLIC OF KOREA
**   INHA UNIVERSITY, INCHEON, REPUBLIC OF KOREA
***   CHUNGNAM NATIONAL UNIVERSITY, DAEJEON, REPUBLIC OF KOREA

Corresponding author: ktpark@kitech.re.kr

anode occurs as per eq. (1), and the reaction occurring at cathode is shown by eq. (2).

$$In_{(l)} \rightarrow In_{(aq)}^{3+} + 3e^- \qquad (1)$$

$$In_{(aq)}^{3+} + 3e^- \rightarrow In_{(l)} \qquad (2)$$

In addition, we observed the current density by changing the content of InF$_3$ used as the initiator, and confirmed the optimum InF$_3$ content by using the Randles-Sevick equation to find the difference in diffusion coefficients. Chronopotentiometry experiments were conducted to observe the change in voltage with time at a constant current density, and to collect In metal, and we could obtain the refining efficiency and the optimum current density.

2. Experiment

Herein we performed molten salt electrorefining of indium from indium-tin (In-Sn) crude metal. A eutectic mixture of lithium fluoride (LiF, 99+%, Strem Chemicals, Inc., USA) and potassium fluoride (KF, 99% crystalline, Thermo Fisher Scientific Inc., USA) was used as the electrolyte and indium fluoride (InF$_3$, >99.9%, Daejung Chemical and Metals Co., Ltd., South Korea) was added as the initiator. Due care was taken to avoid contamination by oxygen and water during the experiment: the apparatus for electrorefining In was installed in a glove box, in which the concentrations of oxygen and water were maintained at less than 10 ppm by continuously purging with Ar.

2.1. Apparatus

The molten salt electrorefining system is shown schematically in Fig. 1. The outermost part of the apparatus (colored green) is made of stainless steel. Three holes were made through the five-layer insulation plate on the cover of the electrolytic cell to provide connectivity to anode, reference electrode, and cathode. The lowest layer of the insulation plate was made of Ni to prevent corrosion of the insulation plate whereas the remaining four layers were made of stainless steel. The electrodes were placed in alumina tubes to prevent short circuit between the electrodes and the insulation plate. The crucible for electrorefining In-Sn crude metal is divided into the outer crucible and the inner crucible. The outer crucible was made of Ni with installed capacity of ~2 kg of molten salt. The two inner crucibles made of Al$_2$O$_3$ were placed inside the outer crucible, one acting as anode (In-Sn liquid metal) and other as collector. Recovered In will be collected inside the crucible.

An anode connector with hollow cross-section was used for continuous insertion of In-Sn metal in liquid anode. A ceramic plate was also installed at the bottom of the crucible assembly to prevent short circuit of the equipment.
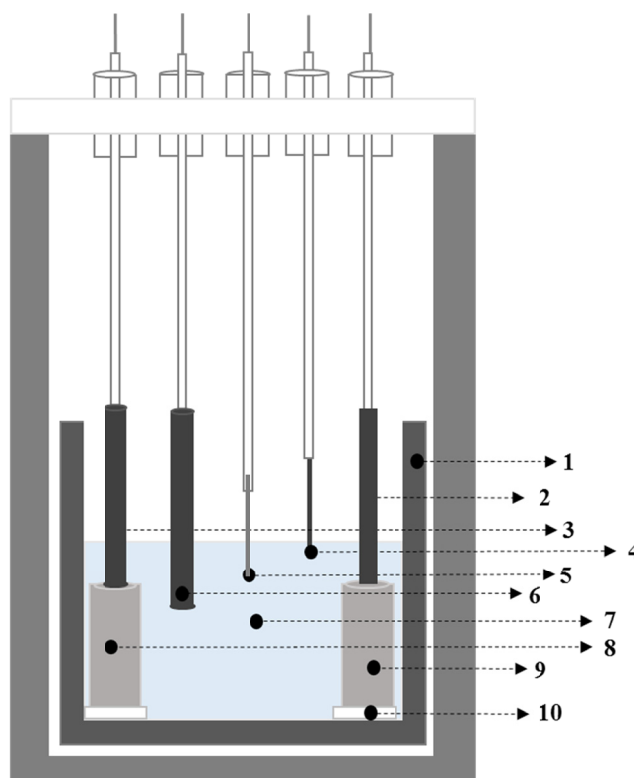
1. Outside crucible (Ni) 2. Cathode current inducer (Mo plate) 3. Anode current inducer (W rod)
4. Working electrode for CV analysis (W wire) 5. Reference quasi electrode (Ni wire)
6. Counter electrode for CV analysis (W rod) 7. KF-LiF utectic electrolyte + αInF$_3$
8. Crucible of impure In-Sn alloy 9. Cathode collector In(Sn) metal 10. Ceramic plate(Al$_2$O$_3$)

Fig. 1. Schematic illustration of electrolytic cell for cyclic voltammetric (CV) and Chronopotentiometry (CP) analysis

2.2. Cyclic voltammetry

CV studies were conducted to evaluate the electrochemical behavior of the electrolyte in In electrorefining. The reference, working, and counter electrodes used were made of 0.1-mm-diameter Ni wire (Fig. 1.5), 1-mm-diameter W wire (Fig. 1.4), and 15-mm-diameter W rod (Fig. 1.6), respectively. Contact length of the electrolyte and the working electrode was set at 10 mm during CV analysis. A LiF-KF eutectic mixture (LiF:KF = 49:51 mol%; melting point, 492°C), weighing 776.4492 g, was used as the electrolyte. To ensure complete melting of LiF-KF, the temperature was set at 700°C (about 200°C higher than the eutectic temperature of LiF-KF). The voltage and current of the electrodes were also controlled using a potentiostat (VSP-300, Bio-Logic Science Instruments, France). After determining the reduction potential of the electrolyte using blank CV experiment, the InF_3 initiator (5-8 wt.%) was added to the electrolyte, and the optimum concentration of the initiator was confirmed.

2.3. Chronopotentiometry

CV analysis was performed to determine the redox potential of the In metal and the electrolyte. For chronopotentiometry, 7 wt.% InF_3 initiator was added to the electrolyte. Polarization behaviors of the anode and cathode were measured by applying a constant current density, and then the In electrodeposition experiments were conducted. Electrolytic cell made of Al_2O_3 crucible, having a diameter of 34 mm and a height of 38 mm, was used which can contain ~300 g of In-Sn liquid metal inside the Ni crucible (Fig. 1.8). In order to prevent misplacement of the internal alumina crucibles in the electrolyte, a fixing base of Ni was used. In-Sn crude metal (110 g, 90wt% In-10wt% Sn) was charged and used as an anode in liquid form. The anode connector was replaced with a 15-mm-diameter W rod (Fig. 1.3) and a Mo plate (15 mm × 3 mm × 220 mm) was used as cathode (Fig. 1.2).

Another alumina crucible was installed below the cathode, such that the In metal recovered from the cathode surface during In electrodeposition can be collected in liquid state (Fig. 1.9). The reference electrode, a 0.1-mm-diameter Ni wire, was a quasi-electrode (Fig. 1.5).

The schematic diagrams of the electrolytic cell and the actual electrode configuration are shown in Fig. 1. The electrodeposit was analyzed by X-ray diffraction (XRD) studies, and the microstructures were analyzed by scanning electron microscopy (SEM) and energy-dispersive X-ray spectroscopy (EDS). Further, inductively coupled plasma-optical emission spectrometry (ICP-OES) analyses were conducted on the electrodeposit and the electrolyte to confirm the impurity content.

3. Results and discussion

The redox potential of the electrolyte was determined by CV analysis to confirm the applicable voltage range. In fluoride-based molten salt, it is difficult to use a conventional reference electrode due to the high reactivity of the molten salt. Therefore, a quasi reference electrode was used, which is expected to produce some errors in measuring the constant oxidation and reduction potentials due to the experimental environment. The scan rate used in the CV experiments was 100 mV/s. The cyclic voltammograms for the blank salts (Fig. 2(a)) were recorded over a potential range of 0 V to −2.75 V vs. reference electrode, and the electrolyte was decomposed at −1.6 V (vs. Ni). The LiF-KF eutectic salt was used as a high-purity electrolyte in consideration of the influence of impurities, and no current peak was observed due to impurities. LiF-KF eutectic electrolyte have been widely used as a electrolyte for electrorefining process and especially active and noble element like Ta, rare earth, Zr and etc commercially electro-refined under fluoride electrolyte containing LiF-KF eutectic composition [10,13-14].

CV analyses were performed by varying the concentration of InF_3 initiator (from 5 wt% to 8 wt%) added to the electrolyte for efficient Indium deposition; the results are shown in Fig. 2(b). Fig. 2(b) shows single reduction behavior from In^{3+} to In. The reduction peak of In^{3+} was observed at −0.1 V (vs. Ni) and the corresponding oxidation peak was also observed. With increasing InF_3 content, the current density increased, and reached saturation at 7 wt% InF_3.

Each peak current and concentrations were used in the Randles-Sevick equation [15] to determine diffusion coefficient of the target element in molten salt electrolysis.

$$i_p = 0.4463 \cdot n \cdot F \cdot A \cdot C \sqrt{\frac{n \cdot F \cdot \upsilon \cdot D}{R \cdot T}} \qquad (3)$$

In equation (3), n is the number of electrons transferred in the reaction, i_p is the peak current, F is the Faraday's constant (96500 C/mol), A is the cross-sectional area of the electrode (cm^2), C is the concentration of In^{3+} (mol/cm^3), D is the diffusion coefficient (cm^2/s), R is the universal gas constant (8.314 J/mol*K), T is the absolute temperature (K), and υ is the scan rate (mV/s).

The diffusion coefficients were found to be 4.28×10^{-8} cm^2/s, 4.512×10^{-8} cm^2/s, 4.85×10^{-8} cm^2/s, and 3.278×10^{-8} cm^2/s for InF_3 concentrations of 5 wt%, 6 wt%, 7 wt%, and 8 wt%, respectively. The highest values of i_p and diffusion coefficient were obtained for 7 wt% of InF_3, and decreased for higher concentrations. Therefore, the concentration of the initiator was fixed at 7 wt% for subsequent experiments.

Before electrorefining, polarization analysis was conducted by chronopotentiometry (CP). Fig. 3 shows the measured potential change by varying the current density. Both anodic and cathodic potentials were found to increase steadily with increasing current density.

In this system, the current density was related to the cathode surface area. The applied current density was stable up to 25 mA/cm^2. However, when the current density exceeded 25 mA/cm^2, the potential was close to −1.6 V, which is the electrolyte decomposition voltage. We used current densities of 5 (condition no. 1), 10 (condition no. 2), and 15 mA/cm^2 (condition
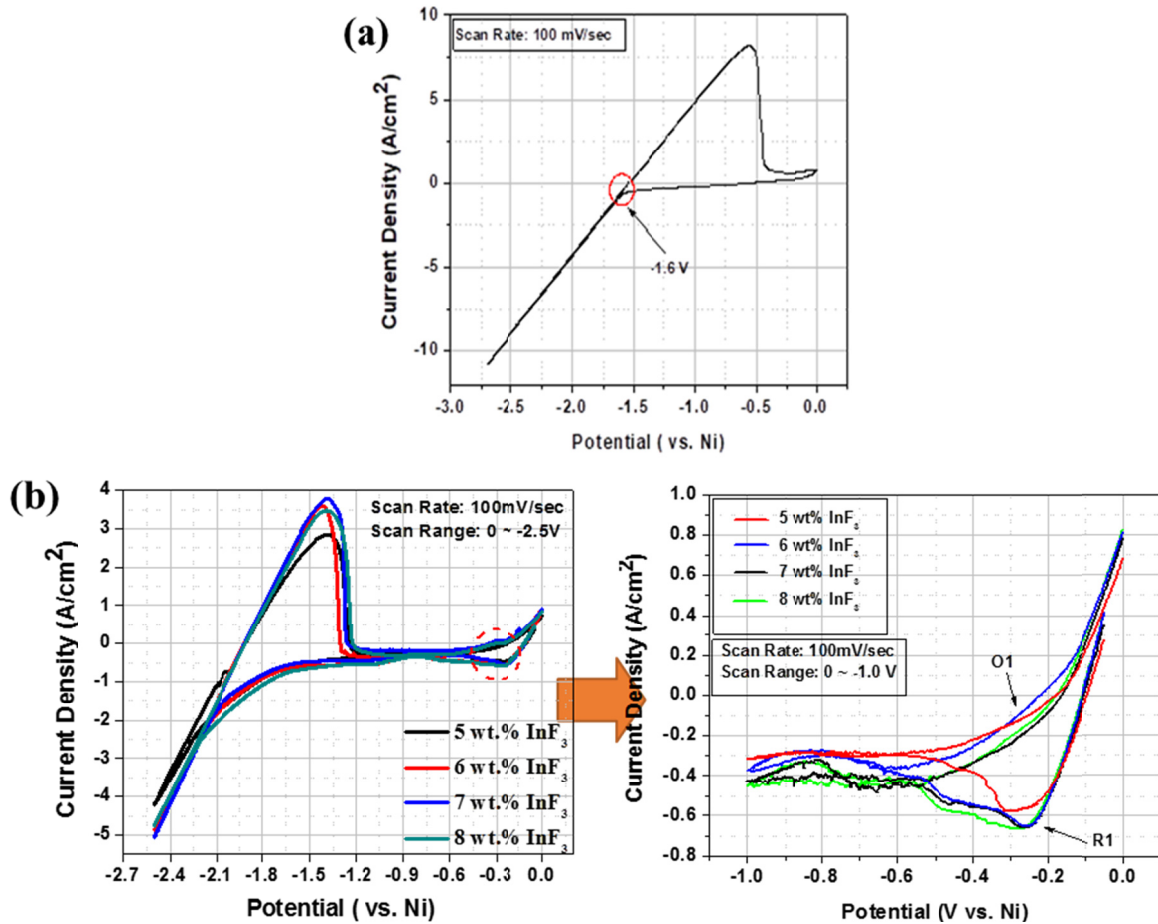
Fig. 2. Cyclic voltammograms obtained using LiF-KF (49:51 mol %) eutectic salt electrolyte, the operating temperature was 700°C, Ni wire (reference electrode), W rod (counter electrode), W wire (working electrode), Scan range 0-2.75 V, Scan rate 100 mV/s (a) 0 wt.% InF_3 initiator (b) 5-8 wt.% InF3 initiator
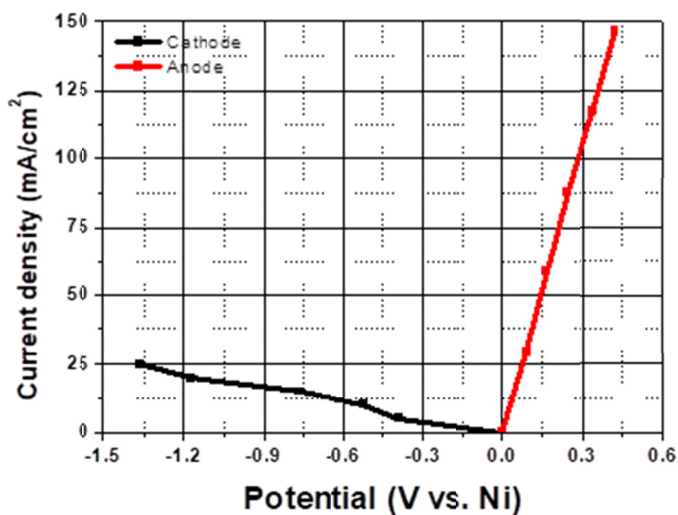

Fig. 3. Polarization curve obtained using an outer crucible (Ni), inner crucible (Alumina), LiF-KF (49:51 mol%) eutectic salt electrolyte, 7 wt.% InF_3, the operating temperature was 700°C, In-Sn alloy (In 90 wt%, Sn 10wt%, Anode), Ni wire (Reference Electrode), Mo Plate (Cathode)

no. 3) because above 15 mA/cm^2, overpotential was obtained, which is not recommended. The conditions No. 3, No. 2, and No. 1 were applied in order.

Based on the above polarization curves, the voltage and current changes on the anode and the cathode, along with the chronopotentiometry analysis results for In metal refining are shown in Fig. 4.

When the open circuit potential (OCP) was measured for the first time, the anode OCP under conditions No. 3, 2, and 1 were between −0.01 V and −0.03 V, between 0.08 V and −0.003 V, and between 0.1 V to 0.06 V, respectively. The corresponding cathode OCP values were between −0.18 V and −0.97 V, between −0.37 V and 0.86 V, and between −0.32 V and −0.61 V, and the voltage drop was observed while In metal was reduced on the Mo plate.

As for the overall voltage behavior, the anode voltage was unstable for up to 5 h. After 5 h, voltage became stable, which means that stable electrolysis occurred. Overpotential was observed under condition no. 3, and not under conditions 1 and 2. The solid electrode was changed or dissolved upon applying an external electrochemical force. In this system, the liquid metal electrode has the advantage of reducing overpotential, compared with processes involving typical solid electrodes [10].

Under all conditions, the In^{3+} ions were reduced and liquefied on the surface of the Mo plate cathode for up to 5 h. Surface area of the electrode was changed, and the voltage change was unstable. However, after 5 h, the entire Mo plate surface area was covered with the reduced In. The surface area of the electrode did
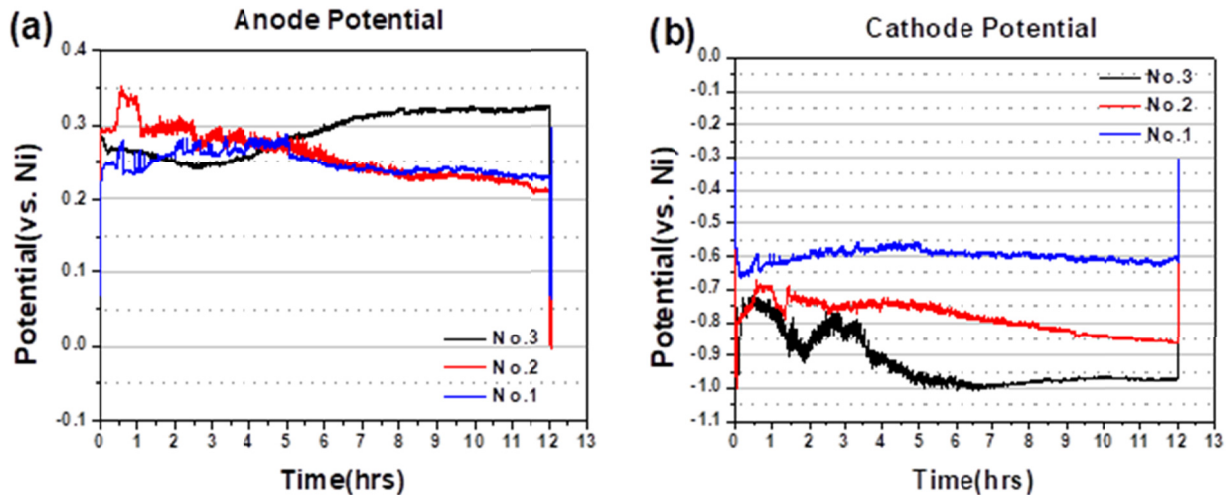
Fig. 4. Chronovoltammogram under various conditions using outer crucible (Ni), inner crucible (Alumina), LiF-KF (49:51 mol%) eutectic salt electrolyte, 7 wt.% InF_3 initiator, the operating temperature was 700°C, In-Sn alloy (In 90 wt%, Sn 10wt%, Anode), Ni wire (Reference Electrode), Mo Plate (Cathode), Cathode current densities were 5, 10, and 15 mA/cm^2 (No. 1, 2, and 3, respectively)
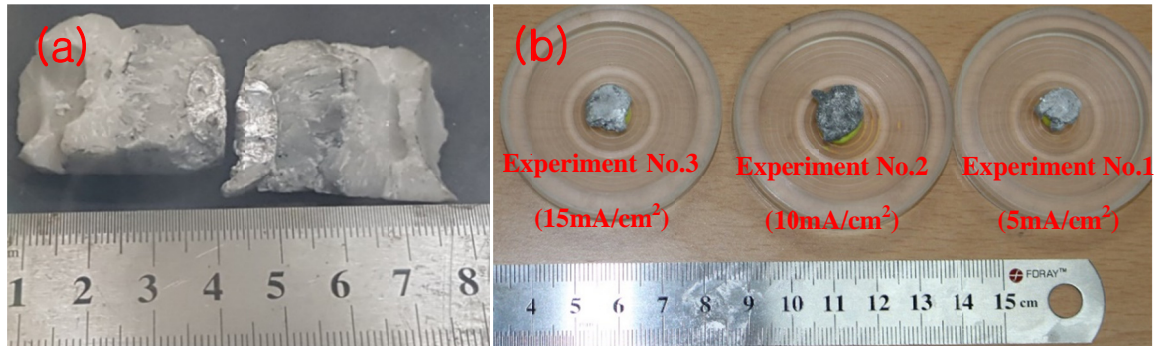

Fig. 5. Images of cathode deposit: (a) Image of cathode deposits produced condition No. 3 (15 mA/cm^2) (b) Images of cathode deposits produced under conditions No. 1, No. 2, No. 3 via washing with D.I. water

TABLE 1

Details of CP conditions for In-Sn electrorefining and units of measurement

Experiment (No.)	Applied current (A)	Holding time (h)	Cathode Current density (mA/cm^2)	Electrochemical method	Electrode	Electrolyte Composition	Analysis
1	0.2		5		Anode: In-Sn (In 90wt%, Sn 10wt%) Cathode: Mo plate	LiF-KF eutectic + 7 wt% InF_3	FE-SEM, EDS, XRD, ICP-OES
2	0.4	12 h	10	Chrono-potentiometry			
3	0.6		15				

not change further, and the cathode deposits fell into the Al_2O_3 crucible, after which the potential was stabilized.

As shown in Fig. 5, most of the deposit was separated physically and the electrolyte was removed without further processing. The remaining electrolyte and impurities floating over the indium melt were also removed, and the surface area of the deposit was increased physically.

The FE-SEM and EDS analyses revealed the microstructure of the electrodeposit, which showed many pores on the surface (Fig. 6). There was no meaningful difference in the microstructures of the samples under different experimental conditions, because In was liquefied and collected after reduction.

KF peaks were detected in the XRD patterns of the samples under conditions No. 2 and No. 3, because the electrolyte was not removed completely (Fig. 7). XRD analysis revealed that only In metal was deposited without any other impurities under condition No. 1. Under all conditions, the oxygen concentration in the glove box was 10 ppm or less, and no oxide was detected in the cathode deposit. The initial electrolyte and the relatively stable samples No. 1 and No. 2 were analyzed to observe impurity, and the results are given in Table 2.

ICP-OES analysis was performed on the electrolyte before the experiment, and on the electrolyte and the deposit after experiment under conditions No. 1 and 2. Samples with relatively stable potentials, i.e. samples No. 1, and No. 2, having different current densities, were selected. Impurity analysis was performed on the electrolyte and the cathode deposits. The reduction potentials for elemental Mn, Si, and Al (vs. Ni) were
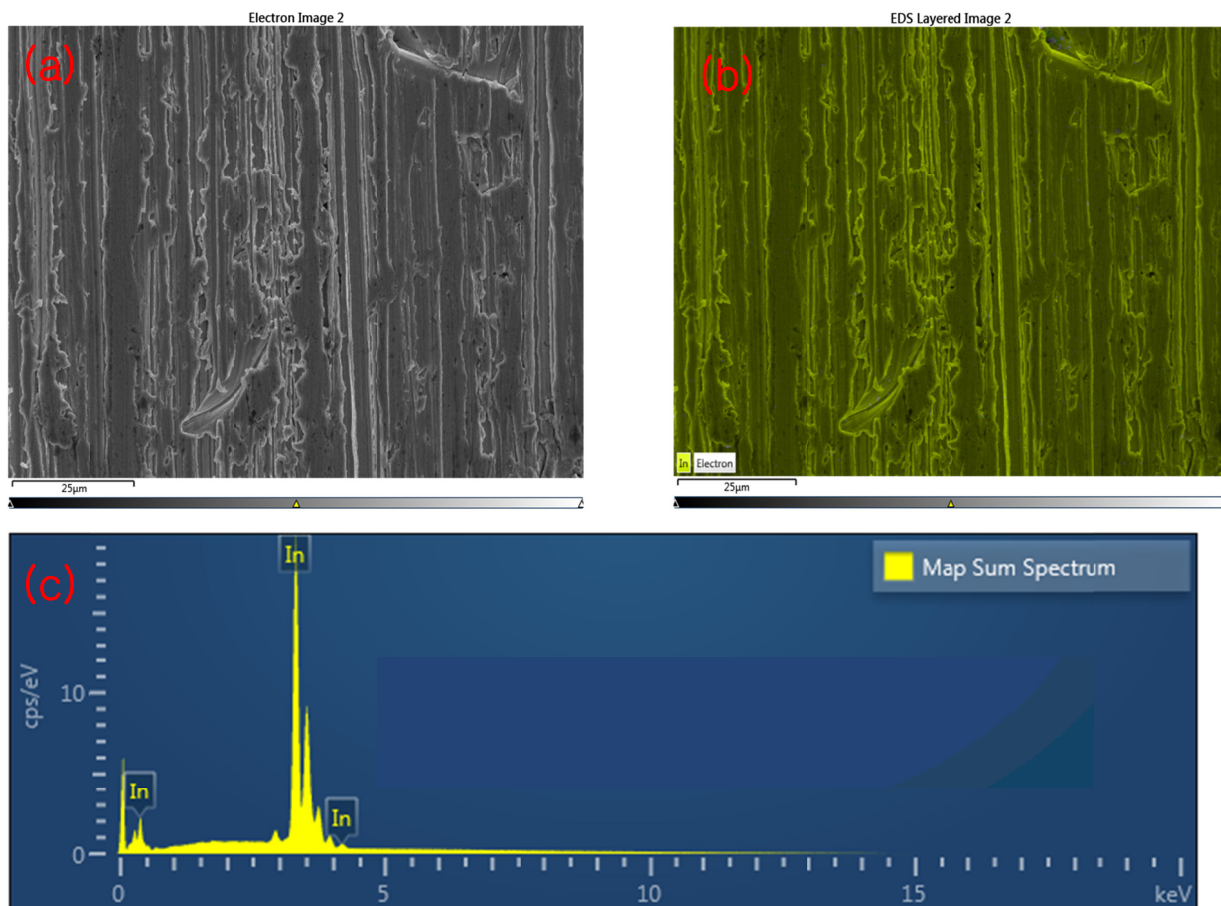
Fig. 6. SEM image of the deposit. General view of deposit produced under condition No. 3: (a) SEM image of cathode deposit surface morphology (b) EDS mapping image of cathode deposit surface morphology (c) EDS mapping result of cathode deposit surface morphology
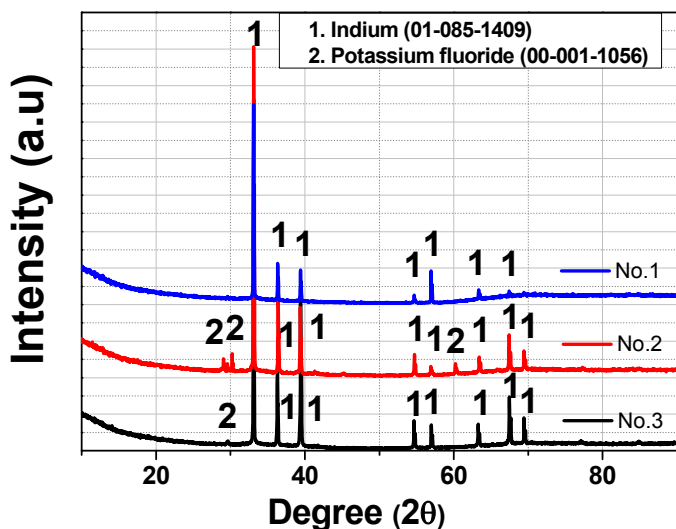

Fig. 7. Comparisons of XRD peaks for Indium deposits under electrorefining conditions No. 1 to No. 3
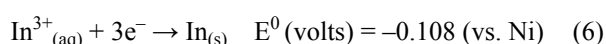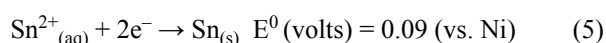
−0.94 V, −0.85 V, and −1.47 V, respectively. Chronopotentiometry showed that the potential varied between −0.69 V and −1 V and between −0.55 V and −0.65 V (vs Ni) for conditions No. 2 and No. 1, respectively. Therefore, the reduction potential values of the three impurity elements, Mn, Si, and Al, were reached under neither condition No. 2 nor condition No. 1. Therefore, these impurities were observed only in the electrolyte, and not in the deposit. Oxidation potential of W was 0.47 V (vs. Ni). The anode potentials in the chronopotentiometry experiment were 0.21-0.35 V and 0.24-0.28 V (vs. Ni) under conditions No. 2 and No. 1, respectively. Therefore, W did not reach the reduction potential values of the three impurity elements, and thus, the W rod was not ionized but was mixed with the electrolyte as a particle-type impurity. Chemical analysis revealed that W was present in the electrolyte, but only small quantities were detected in the cathode deposit. The cathode material Mo underwent some diffusion into the deposit as expected because the process temperature was set at 700°C. Current density was not applied to the outer crucible; therefore, Ni was not dissolved electrochemically, but was already present in the raw electrolyte as impurity. Ni was expected to be electrodeposited at the cathode because the reduction potential of Ni is 0 V (vs. Ni) and the cathode potential is less than −0.5 V under all experimental conditions. W and Ni require further analysis and consideration. The redox potentials of Sn and In^{3+} were found to be 0.09 V and −0.108 V (vs. Ni), respectively, as shown in equation (5). The redox potential of Sn was a little different from the indium redox potential, which was found to be electrodeposited during the indium electrorefining experiment. Although 10 wt% Sn was present in the In-Sn anode, the content of Sn at the deposit, observed by ICP-OES, was 1.5 wt%, which was very small

Level of impurity in indium metal, electrolyte of electrorefining

Conditions	Sample	Elements (ppm)						
		Mn	Mo	Ni	Si	Al	W	Sn
Raw LiF-KF	Salt	251	70	497	34130	4002	1286	0.5
No. 2 (10 mA/cm^2)	Salt	110	73	1	2351	4356	10150	134
	Deposit	0	691	558	0	14	121	15330
No. 1 (5 mA/cm^2)	Salt	170	65	8	2653	4935	9920	11
	Deposit	0	134	270	1	20	24	15960

compared to the initial concentration. Thus, a refining effect was confirmed, and the suggested process was successful in electrorefining indium from In-Sn alloy.

$$Sn^{2+}_{(aq)} + 2e^- \rightarrow Sn_{(s)} \quad E^0 \text{ (volts)} = 0.09 \text{ (vs. Ni)} \quad (5)$$

$$In^{3+}_{(aq)} + 3e^- \rightarrow In_{(s)} \quad E^0 \text{ (volts)} = -0.108 \text{ (vs. Ni)} \quad (6)$$

4. Conclusions

Experiments were conducted to refine In metal by a molten salt electrolytic system. Varying amounts of InF_3 was added to a LiF-KF eutectic salt, and cyclic voltammetry was performed. With increasing InF_3 concentration, the applicable current density increased, reaching saturation at ~7 wt% InF_3. Electrolytic refining was performed at a current density less than 25 mA/cm^2 because eutectic salt decomposition starts above 25 mA/cm^2. Three current densities of the cathode surface area were used in the chronopotentiometry experiment. SEM and EDS analyses of the recovered electrodeposits showed pure In metal with many pores. XRD results showed that the recovered In metal contained no oxygen. Single-phase In metal was observed at current density of 5 mA/cm^2. However, at 15 mA/cm^2, and 10 mA/cm^2, In metal together with the remaining electrolyte was observed. In the cathode deposit, 134 ppm Mo, 270 ppm Ni, 24 ppm W, and 20 ppm Al were observed, and no Mn and Si were observed. ICP-OES analysis showed that 5 mA/cm^2 current density is the ideal condition for electrorefining In metal from In-Sn 10 wt% alloy.

REFERENCES

[1] M. Lokanc, R. Eggert, M. Redlinger, The Availability of Indium: The Present, Medium Term, and Long Term, NREL Technical Monitor: Michael Woodhouse. NREL/SR-6A20-62409 October 2015.

[2] M.T. Dang, G. Wantz, L. Hirsch, J.D. Wuest, Thin Solid Films **638**, 236-243 (2017).

[3] K. Zhang, Y. Wu, W. Wang, B. Li, Y. Zhang, T. Zuo, Resour. Conserv. Recycl. **104**, 276-290 (2015).

[4] O. Takeda, K. Nakano, Y. Sato, Mater. Trans. **55** (2), 334-341 (2014).

[5] G.Z. Chen, D.J. Fray, T.W. Farthing, Nature **407**, 361-364 (2000).

[6] X.Y. Yan, D.J. Fray, Metall. Mater. Trans. B **33**, 685-693 (2002).

[7] A. Girginov, T.Z. Tzvetkoff, M. Bojinov, J. Appl. Electrochem. **25**, 993-1003 (1995).

[8] C. Scordilis-Kelley, J. Fuller, R.T. Carlin, J. Electrochem. Soc. **139** (3), 694-699 (1992).

[9] B.P. Reddy, S. Vandarkuzhali, T. Subramanian, P. Venkatesh, Electrochim. Acta **49**, 2471-2478 (2004).

[10] K.T. Park, T.H. Lee, N.C. Jo, H.H. Nersisyan, B.S. Chun, H.H. Lee, J.H. Lee, J. Nucl. Mater. **436**, 130-138 (2013).

[11] Y. Sakamura, T. Hijikata, K. Kinoshita, T. Inoue, T.S. Storvick, C.L. Krueger, L.F. Grantham, S.P. Fusselman, D.L. Grimmett, J.J. Roy, J. Nucl. Sci. Technol. **35**, 49-59 (1998).

[12] J. Cai, X. Luo, G.M. Haarberg, O.E. Kongstein, S-I. Wang, J. Electrochem. Soc. **159** (3), D155-D158 (2012).

[13] C. Hamela, P. Chamelot, P. Taxil, Electrochim. Acta. **49**, 4467-4476 (2004).

[14] S.L. Lee, M. Cipollo, D. Windover, C. Rickard, Surf. Coat. Technol. 120-121, 44-52 (1999).

[15] C. Donath, E. Neascu, N. Ene, Rev. Roum. Chim. **56** (8), 763-769 (2011).